Proceedings of the 27th International Conference on Automation & Computing, University of the West of England, Bristol, UK, 1-3 September 2022

Rapid State of Health Estimation of Lithium-ion Batteries based on An Active Acoustic Emission Sensing Method

Zuolu Wang[1], Kaibo Lu[2], Xun Chen[3], Dong Zhen[4], Fengshou Gu[1,*] and Andrew D. Ball[1]

[1]Centre for Efficiency and Performance Engineering, University of Huddersfield, Huddersfield, HD1 3DH, UK.
[2]College of Mechanical Engineering, Taiyuan University of Technology, Shanxi 030024, PR China.
[3]General Engineering Research Institute, Liverpool John Moores University, Liverpool L3 3AF, UK.
[4]Tianjin Key Laboratory of Power Transmission and Safety Technology for New Energy Vehicles, School of Mechanical Engineering, Hebei University of Technology, Tianjin, 300401, P. R. China.
*Corresponding author: E-mail address: f.gu@hud.ac.uk

2022 27th International Conference on Automation and Computing (ICAC) | 978-1-6654-9807-4/22/$31.00 ©2022 IEEE | DOI: 10.1109/ICAC55051.2022.9911094

***Abstract*—Lithium-ion batteries have widely used as the power sources of electric vehicles (EVs). Accurate and rapid state of health (SOH) estimation in the battery management system (BMS) plays an essential part in improving the reliability and safety of electric systems. This paper develops an active acoustic emission (AE) sensing technology for non-intrusive and rapid battery SOH estimation. The proposed method takes consideration into the changing internal battery material properties under different levels of degradation. In this method, the power ultrasound is used to propagate into the layered battery and excite different AE events of the battery under different cycles. The AE transducer from the opposite side of the battery can actively sense the elastic waves that reflect the life status. This allows more state information to be captured in a wide frequency band for effective SOH estimation. The results indicate that the RMS of the AE signal can be indicative of battery SOH, and the frequency band 270-300 kHz can provide a more linear SOH estimation under various discharging stages. It is validated that the developed technique can achieve rapid and reliable SOH estimation of lithium-ion batteries.**

Keywords- Lithium-ion battery; state of health; material properties; active acoustic emission; power ultrasound

I. INTRODUCTION

In order to alleviate the enormous pressure brought by the increasing consumption of fossil energy and propose solutions to climate change, energy storage systems and electric vehicles (EVs) have been extensively developed [1]. Lithium-ion batteries have developed into dominant energy storage units thanks to their higher power efficiency and lower self-discharge rate [2]. The battery state of health (SOH) can deliver the percentage of the current maximum available capacity to its nominal capacity, which indicates the aging level of the battery [3]. Accurate SOH estimation can result in a reliable battery management system (BMS) for improving the safety, battery performance and even extending the battery lifespan. Thus, developing an accurate and efficient SOH estimation method is still challenging and promising work for practical applications.

Currently, the battery's SOH estimation has attracted extensive attention. In [4], the authors have given a comprehensive review on the battery SOH estimation approaches that can be generally grouped into three categories, including model-based, data-driven, and advanced sensing-based methods.

Model-based SOH estimation is implemented through modelling the battery parameters. The electrical equivalent circuit model (EECM) and electrochemical model (EM) are two popular models for accessing the battery SOH. In EECM, some essential variables, including polarization resistance/capacitance and internal ohmic resistance, vary with cycling and they are commonly used to characterize the battery SOH. Many filtering algorithms, such as EKF [5], PF [6], and AEKF [7], have been proposed for the identification of electrical parameters and the accurate SOH estimation. The EM considers the actual electrochemical reactions inside the battery, such as the solid-phase/liquid-phase diffusion process [8]. For example, Pseudo-Two-Dimensional (P2D) model and single particle model (SPM) [9] are two typical electrochemical models for presenting the dynamics of the battery, in which the active material concentration can be an effective factor to characterize the battery SOH. From different perspectives, both EM and EECM can duplicate the battery's characteristics, but the large computational equations undoubtedly increase the complexity of state estimation.

The implementation of the data-driven approach is like a black box system that does not need to consider the complex electrochemical characteristics, and it only focuses on the relationship between the measured battery variables (e.g., voltage, current, and temperature) and degraded capacity for SOH prediction [10]. Due to the powerful nonlinear modelling, a variety of machine learning methods, such as the hybrid neural network that combines gate recurrent unit and convolutional neural network (GRU-CNN) [11], variable length input long-short term memory (VLR-LSTM) network [12] and hybrid kernel function relevance vector machine (HKRVM) [13], have been employed to SOH evaluation of the battery. However, the data-driven method has high requirements on both computing power and large battery degradation datasets for various working conditions. This undoubtedly brings a huge challenge to the BMS due to its limited storage space and computing power.

Recently, some advanced sensing-based technologies have been developed and prove effective for more

convenient battery SOH evaluation. For example, electrochemical impedance spectroscopy (EIS) has been demonstrated effective to monitor the internal impedance under different cycles through the high frequency AC current excitation [14]. However, the acquisition of the impedance spectrum across a broad range of frequency excitations can increase the computational costs. Moreover, monitoring ultrasound technology is performed for SOH detection by focusing on the changes of battery material properties. Paper [15] proposed the ultrasonic pulse for the battery SOH estimation for the first time. It indicates that two parameters, including time of flight (TOF) and signal amplitude (SA) of the pulse echo, are highly correlated with battery SOH. Based on the variation of SA and TOF in the ultrasonic pulses, many studies have dedicated to SOH estimation [16], [17]. It is expected that the monitoring methods that take accounts into the battery material properties under different cycles can achieve easy, rapid, and accurate SOH estimation. However, the current widely used ultrasound-based methods are based on the single frequency pulse. Consequently, only a small amount of information can be considered for battery SOH evaluation.

In view of the changes of the battery material properties, this paper proposes an active acoustic emission (AE) sensing technology to achieve the rapid and cost-effective lithium-ion battery SOH estimation for the first time. The developed rapid detection method involves two main modules, including power ultrasound and AE. In particular, the proper power ultrasound is propagated to the layered battery and hence trigger elastic waves under different degradations. A wide AE transducer from the opposite side of the battery is applied to actively track the released elastic pulses that can characterize the battery life status. The experimental results indicate that the RMS of the AE signal can be easily calculated for the effective SOH estimation. The frequency band 270-300 kHz, around the 7th harmonics of the excitation frequency, can effectively provide battery SOH estimation at various discharging stages.

The rest of this paper is shown as follows: Section 2 introduces the proposed monitoring method in detail. Section 3 presents the experimental setup and detailed test procedures. The SOH estimation results from the experimental studies are presented in Section 4. Conclusions are presented in Section 5.

II. TEST THEORY

A. Multi-layered Structure

The pouch lithium-ion battery mainly consists of cathode, anode, and electrolyte [18], [19]. Thus, it is a multi-layered structure. The anode and cathode are coated on copper foils and aluminum, and they are divided by the separator as illustrated in Fig. 1.

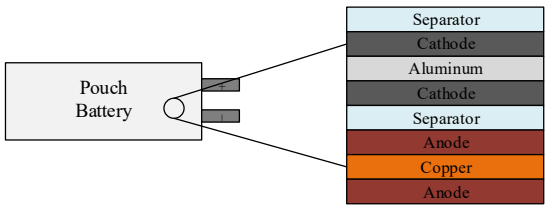

Figure 1. Multilayered structure of the pouch battery.

Various layered materials have different properties and hence cause a variety of acoustic impedances. Different degrees of transmissions and reflections are induced when sound waves pass through two different materials. The reflection coefficient is expressed as [20]:

$$R = \frac{Z_2 - Z_1}{Z_2 + Z_1} \quad (1)$$

$$Z = \rho c \quad (2)$$

where Z_1 and Z_2 denote the acoustic impedance of two different battery materials. c denotes the wave velocityand ρ represents the density. The reflection coefficient is between 0 and 1, while $1 - R$ stands for the transmission coefficient.

Battery material properties change as the battery degrades. Long-term cycling will consume the active material, which can result in the formation of solid electrolyte interphase and the loss of lithium ions. Experimental results have revealed that the elastic modulus and density of the electrode material decreased with the number of cycles [21]. Therefore, these irreversible changes in material properties can alter the reflection coefficient R, which can influence the propagation of sound waves and introduce different levels of attenuation of sound transmission in batteries.

B. Proposed Active AE Sensing Method

The battery SOH can be treated as the function of the battery material properties. The proposed monitoring method combines the applications of AE and power ultrasound, which is to sense the changes in the material properties and then characterize the battery SOH. Compared to the ultrasonic sensor, the AE sensor can achieve broadband monitoring and hence collect more adequate information for SOH estimation of the lithium-ion battery.

The appropriate power ultrasound is applied to excite the battery and trigger different elastic waves under different degradations. Its role is included in mechanical and chemical effects on the battery. For example, the mechanical effects, such as shear force and shock wave, can act on the materials inside the battery and trigger different responses. Moreover, mechanical effects can accelerate the movement of lithium ions and thus the chemical reaction. As a result, the proper power ultrasound that passes through the battery with different battery material properties can lead to micro deformations and excite different elastic pulses.

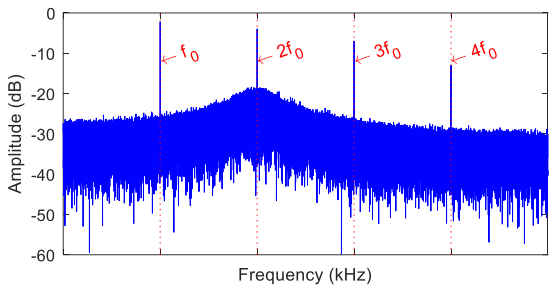

Figure 2. Acoustic emission spectrum with fundamental excitation frequency f_0.

Furthermore, the AE transducer installed on the opposite side of the battery is employed to actively track the released elastic pulses that can characterize the battery life status. Power ultrasound can introduce different AE events as battery material properties change. Thus, the AE sensor can capture the high-frequency waves and achieve the battery SOH estimation. Compared to the traditional vibration or sound sensor, the AE monitoring can effectively acquire the transient waves released by local materials in a high sampling frequency. In addition, more information can be acquired by the AE sensor in a wide frequency band [22]. As shown in Fig. 2, the harmonics of the fundamental frequency and the broadband signal can be obtained if the battery is acted by the excitation source with the fundamental frequency f_0.

III. EXPERIMENTS

A. Test Rig

To validate the performance of the developed technology for rapid battery SOH estimation, the power ultrasound and AE test rig were developed. Fig 3 displays the schematic diagram of the designed test bench. It is composed of AE acquisition system, preamplifier, AE sensor, battery tester, temperature chamber, power ultrasound generator, vibrator, current clamp, data acquisition system, pouch battery, thermocouple, and host computer. The EBC-A20 battery tester satisfies the basic battery test, such as CC discharge, constant power discharge, CC-CV charge, and multi-step cycle test. The electrical parameters, such as terminal voltage, loading current, and surface temperature, are measured by the 16 bit-data acquisition system with sampling frequency of 10 Hz. Fig. 3 (b) displays the layout of the targeted pouch battery in the chamber with constant temperature of 25℃. The thermocouple is adopted to measure the temperature of the battery surface. In the test, the vibrator excited by the ultrasonic generator is installed on the battery surface to excite the battery, in which the excitation frequency of the ultrasonic generator is 40 kHz. The response signal is collected by the AE transducer that can achieve the effective measurement at a wide range of frequency band between 60 kHz-400 kHz. Therefore, the sampling frequency and a digital bandpass filter of the acquisition system are set as 2 MHz and 20 kHz-500 kHz, respectively. The gain of the preamplifier is 40 dB. The experimental pouch battery is presented in Fig. 4 and the specifications are listed in Table 1.

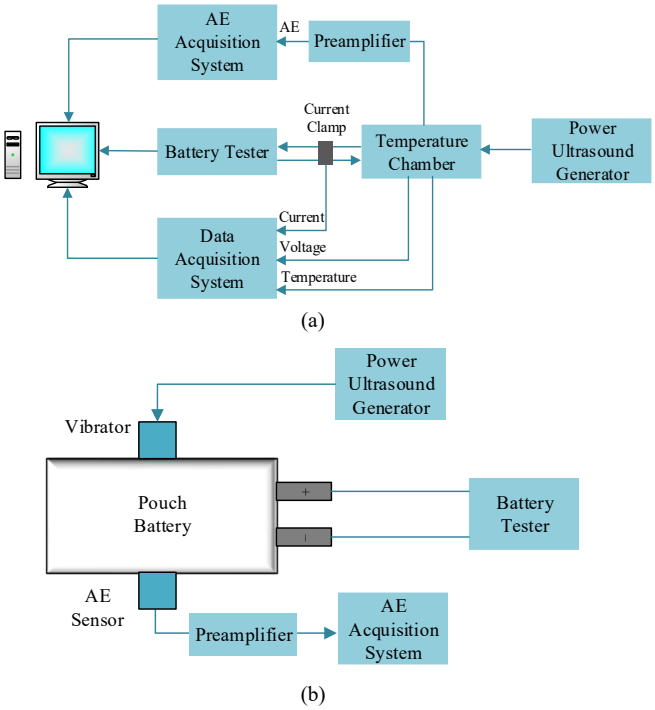

Figure 3. Schematic diagram of (a) power ultrasound and AE test rig, and (b) the layout of the pouch battery in the temperature chamber.

Figure 4. The experimental pouch battery.

TABLE 1. THE LI-ION POUCH BATTERY SPECIFICATIONS.

Item	Specification
Model	Polymer lithium-ion battery
Nominal capacity	2 Ah
Nominal voltage	3.7 V
Charge/discharge cut-off voltage	4.2 V/3 V
Size	7×43.3×62 mm

B. Test Procedures

In the test, both the charging and discharging of the battery are carried out at 0.5 C rate. The cycle test was performed to degrade the battery. The proposed active AE sensing technology was carried out at the interval of 20 cycles. In the test, the battery is excited by the power ultrasound at three different points during the discharging stage, and the AE signals were collected accordingly. Table 2 describes the three points for the operations of ultrasonic excitation and AE signal collection. For each of the operations, the power ultrasound was first input to the battery and lasted for 10 s, and then the AE signal was acquired at the 5th second and the collection lasted for 5 s.

TABLE 2. DESCRIPTION OF TEST TIME POINTS.

Test Points	Description
Point 1	Before discharging: SOC = 100%
Point 2	In discharging: SOC = 50%
Point 3	After discharging: SOC = 0%

Note: State of charge (SOC).

IV. RESULTS AND DISCUSSIONS

A. Time and Frequency Domain Analysis

The battery was degraded to 100 cycles in this test. Fig. 5 illustrates the actual available battery capacity over cycles and the calculated SOH under different cycles. It can be seen that the battery SOH drops to about 96.87% after 100 cycles.

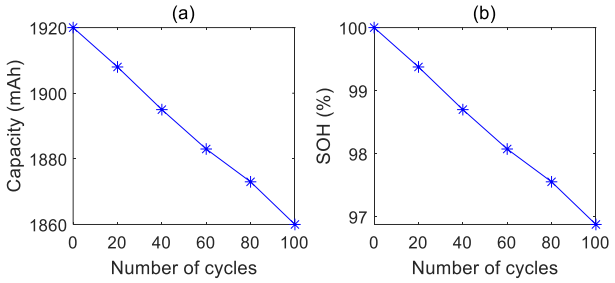

Figure 5. The variation of (a) the actual battery capacity and (b) SOH with cycles.

Take cycle 0 and cycle 20 as an example, Fig.6 shows the time-domain waveforms and their spectra at SOC = 100%. In the time domain waveform, it is found that the signal amplitudes at 20 cycles are a little smaller than that at 0 cycle. However, it is difficult to distinguish between different cycles using the signal amplitudes. All the spectra are shown between 0 kHz to 500 kHz because of the used digital filter in the AE acquisition system. As illustrated in Fig.6 (b) and (d), the frequency components are mainly the harmonics of the fundamental excitation frequency, such as $2f_0$, $3f_0$, $4f_0$, $5f_0$, $6f_0$, and $7f_0$. Therefore, a variety of frequency bands around the harmonics can be obtained. It is assumed that the different frequency bands can present different responses to the changes in the battery materials and even the battery SOH. Finally, the statistical parameter root mean square (RMS) is applied to analyze the AE signal under different frequency bands for the battery SOH estimation.

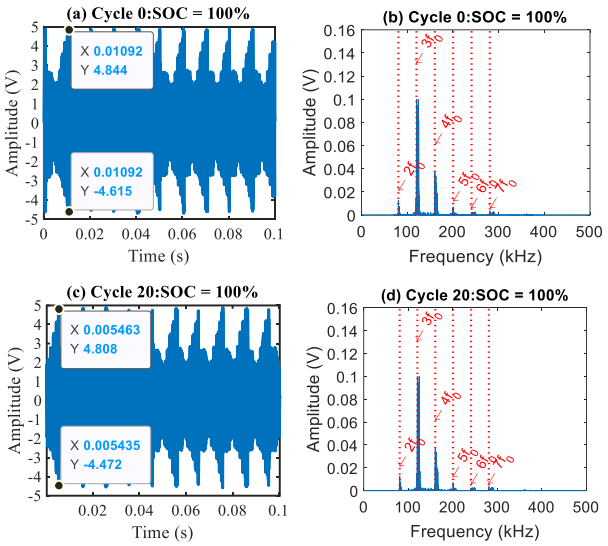

Figure 6. Time-domain waveform at (a) cycle 0 (SOC = 100%), (b) spectrum at cycle 0 (SOC = 100%), time-domain waveform at (c) cycle 20 (SOC = 100%), and (d) spectrum at cycle 20 (SOC = 100%).

B. SOH Estimation

Fig. 7 shows the calculated RMS at three measured points using various frequency bands under different SOHs. It is clear that the different frequency bands present different responses to the battery SOH. As mentioned in Section 2, the battery material properties change with ageing. For example, the density and elastic modulus of the electrode material reduce with the increase of degradation during which many lithium ions are consumed gradually. This can cause the attenuation of sound waves when propagating across the battery. Therefore, the calculated RMS under most of the frequency bands presents a downward trend with the degradation of the battery. As seen in Fig. 7 (a) (b) (c) and (g), the RMS calculated at the three points using the frequency bands, such as 70-400 kHz, 75-90 kHz, 110-150 kHz, and 270-300 kHz, decrease with the decreasing of SOH. However, the calculated results at some measured points using the frequency bands, including 150-180 kHz, 185-215 kHz, and 220-260 kHz, cannot effectively characterize the battery SOH. For example, the RMS of the measured AE signals in 150-180 kHz fluctuates largely and cannot give a linear relationship with battery SOH, which hence cannot offer a reliable battery SOH evaluation.

In contrast, the RMS calculated in 270-300 kHz exhibit a better linear correspondence with SOH at any testing points, as shown in Fig. 7 (g). In particular, Fig. 8 gives the calculated RMS at three testing points in the frequency band 270-300 kHz. It is noted that the RMS can characterize the variation of battery SOH relatively linearly. Therefore, the experimental results validate the feasibility of the designed monitoring method for the fast and convenient SOH evaluation of the lithium-ion battery.

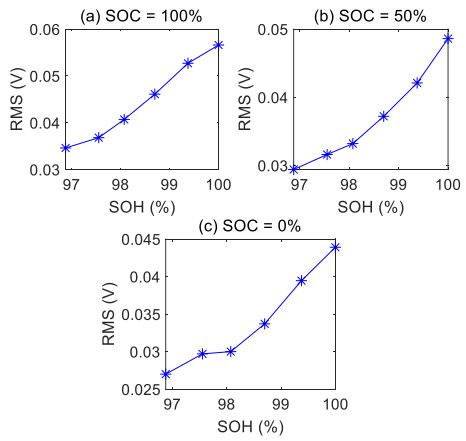

Figure 8. The corresponding relationship between SOH and RMS calculated 0 using the frequency band 270-300 kHz at three measured points (a) SOC = 100%, (b) SOC = 50%, and (c) SOC = 0%.

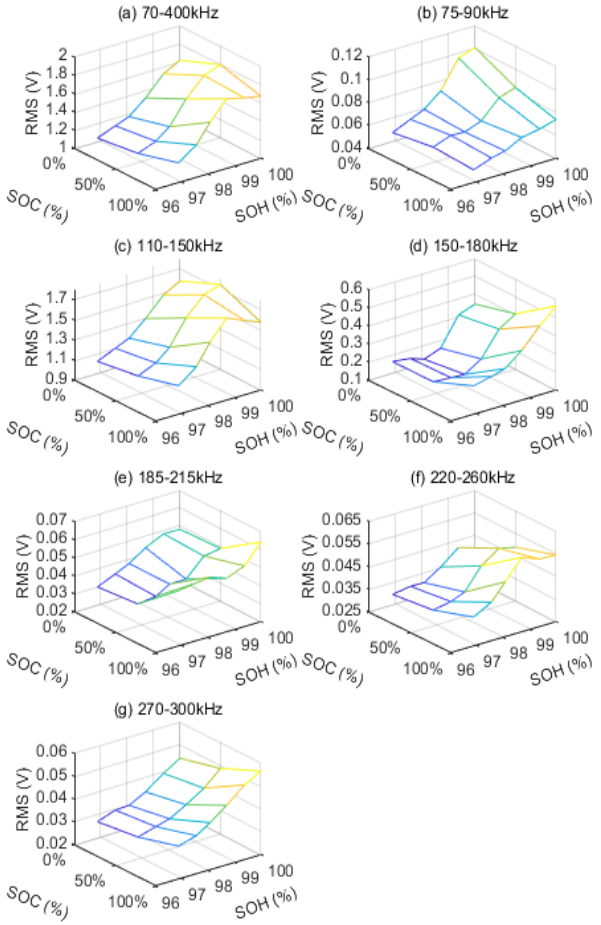

Figure 7. RMS calculated using the frequency band (a) 70-400 kHz, (b) 75-90 kHz, (c) 110-150 kHz, (d) 150-180 kHz, (e) 185-215 kHz, (f) 220-260 kHz, and (g) 270-300 kHz under different SOHs.

V. CONCLUSIONS

This paper developed an active AE sensing technology by focusing on the varying battery material properties with degradations and it can effectively achieve the fast detection of the battery SOH. In this method, the appropriate power ultrasound aims to excite the battery and trigger different AE events under different levels of degradation, and the wide AE sensor can capture more state information in a wide range of frequency band. It is important to mention that the RMS can be an effective indicator for battery SOH estimation. Generally, the calculated RMS under various frequency bands exhibits a decreasing trend with the decrease of SOH. The experiment results reveal that the frequency band 270-300 kHz with $7f_0$ can provide accurate SOH evaluation at three measured points. Therefore, it is validated that the developed monitoring technology can effectively achieve the fast detection of battery SOH.

REFERENCES

[1] Z. Wang, G. Feng, X. Liu, F. Gu, and A. Ball, 'A novel method of parameter identification and state of charge estimation for lithium-ion battery energy storage system', *Journal of Energy Storage*, vol. 49, p. 104124, 2022.

[2] Y. Toughzaoui *et al.*, 'State of health estimation and remaining useful life assessment of lithium-ion batteries: A comparative study', *Journal of Energy Storage*, vol. 51, p. 104520, 2022.

[3] L. Driscoll, S. de la Torre, and J. A. Gomez-Ruiz, 'Feature-based lithium-ion battery state of health estimation with artificial neural networks', *Journal of Energy Storage*, vol. 50, p. 104584, 2022.

[4] Z. Wang, G. Feng, D. Zhen, F. Gu, and A. Ball, 'A review on online state of charge and state of health estimation for lithium-ion batteries in electric vehicles', *Energy Reports*, vol. 7, pp. 5141–5161, 2021.

[5] X. Tan, D. Zhan, P. Lyu, J. Rao, and Y. Fan, 'Online state-of-health estimation of lithium-ion battery based on dynamic parameter identification at multi timescale and support vector regression', *Journal of Power Sources*, vol. 484, p. 229233, 2021.

[6] R. Xiong, Y. Zhang, H. He, X. Zhou, and M. G. Pecht, 'A double-scale, particle-filtering, energy state prediction algorithm for lithium-ion batteries', *IEEE Transactions on Industrial Electronics*, vol. 65, no. 2, pp. 1526–1538, 2017.

[7] H. He, R. Xiong, and H. Guo, 'Online estimation of model parameters and state-of-charge of LiFePO4 batteries in electric vehicles', *Applied Energy*, vol. 89, no. 1, pp. 413–420, Jan. 2012, doi: 10.1016/j.apenergy.2011.08.005.

[8] M.-F. Ge, Y. Liu, X. Jiang, and J. Liu, 'A review on state of health estimations and remaining useful life prognostics of lithium-ion batteries', *Measurement*, vol. 174, p. 109057, Apr. 2021, doi: 10.1016/j.measurement.2021.109057.

[9] Y. Bi, Y. Yin, and S.-Y. Choe, 'Online state of health and aging parameter estimation using a physics-based life model with a particle filter', *Journal of Power Sources*, vol. 476, p. 228655, 2020.

[10] L. Chen, Z. Lü, W. Lin, J. Li, and H. Pan, 'A new state-of-health estimation method for lithium-ion batteries through the intrinsic relationship between ohmic internal resistance and capacity', *Measurement*, vol. 116, pp. 586–595, 2018.

[11] Y. Fan, F. Xiao, C. Li, G. Yang, and X. Tang, 'A novel deep learning framework for state of health estimation of lithium-ion battery', *Journal of Energy Storage*, vol. 32, p. 101741, 2020.

[12] J. Hong, Z. Wang, W. Chen, L. Wang, P. Lin, and C. Qu, 'Online accurate state of health estimation for battery systems on real-world electric vehicles with variable driving conditions considered', *Journal of Cleaner Production*, vol. 294, p. 125814, 2021.

[13] Z. Lyu, G. Wang, and R. Gao, 'Synchronous state of health estimation and remaining useful lifetime prediction of Li-Ion battery through optimized relevance vector machine framework', *Energy*, p. 123852, 2022.

[14] N. Meddings *et al.*, 'Application of electrochemical impedance spectroscopy to commercial Li-ion cells: A review', *Journal of Power Sources*, vol. 480, p. 228742, 2020.

[15] P. Ladpli, F. Kopsaftopoulos, and F.-K. Chang, 'Estimating state of charge and health of lithium-ion batteries with guided waves using built-in piezoelectric sensors/actuators', *Journal of Power Sources*, vol. 384, pp. 342–354, 2018.

[16] R. J. Copley, D. Cumming, Y. Wu, and R. S. Dwyer-Joyce, 'Measurements and modelling of the response of an ultrasonic pulse to a lithium-ion battery as a precursor for state of charge estimation', *Journal of Energy Storage*, vol. 36, p. 102406, 2021.

[17] G. Zhao, Y. Liu, G. Liu, S. Jiang, and W. Hao, 'State-of-charge and state-of-health estimation for lithium-ion battery using the direct wave signals of guided wave', *Journal of Energy Storage*, vol. 39, p. 102657, 2021.

[18] C. M. Costa, E. Lizundia, and S. Lanceros-Méndez, 'Polymers for advanced lithium-ion batteries: State of the art and future needs on polymers for the different battery components', *Progress in Energy and Combustion Science*, vol. 79, p. 100846, 2020.

[19] X. Meng *et al.*, 'Internal failure of anode materials for lithium batteries—A critical review', *Green Energy & Environment*, vol. 5, no. 1, pp. 22–36, 2020.

[20] R. J. Copley, D. Cumming, Y. Wu, and R. S. Dwyer-Joyce, 'Measurements and modelling of the response of an ultrasonic pulse to a lithium-ion battery as a precursor for state of charge estimation', *Journal of Energy Storage*, vol. 36, p. 102406, 2021.

[21] K. Zeng and J. Zhu, 'Surface morphology, elastic modulus and hardness of thin film cathodes for Li-ion rechargeable batteries', *Mechanics of Materials*, vol. 91, pp. 323–332, 2015.

[22] M. Hodnett, R. Chow, and B. Zeqiri, 'High-frequency acoustic emissions generated by a 20 kHz sonochemical horn processor detected using a novel broadband acoustic sensor: a preliminary study', *Ultrasonics sonochemistry*, vol. 11, no. 6, pp. 441–454, 2004.